Mol Genet Genomics (2007) 278:255–271
DOI 10.1007/s00438-007-0246-9

ORIGINAL PAPER

Dissection of the *Bradyrhizobium japonicum* NifA+σ^{54} regulon, and identification of a ferredoxin gene (*fdxN*) for symbiotic nitrogen fixation

Felix Hauser · Gabriella Pessi · Markus Friberg · Christoph Weber · Nicola Rusca · Andrea Lindemann · Hans-Martin Fischer · Hauke Hennecke

Received: 5 April 2007 / Accepted: 7 May 2007 / Published online: 15 June 2007

Abstract Hierarchically organized regulatory proteins form a complex network for expression control of symbiotic and accessory genes in the nitrogen-fixing soybean symbiont *Bradyrhizobium japonicum*. A genome-wide survey of regulatory interactions was made possible with the design of a custom-made gene chip. Here, we report the first use of the microarray in a comprehensive and complete characterization of the *B. japonicum* NifA+σ^{54} regulon which forms an important node in the entire network. Comparative transcript profiles of anaerobically grown wild-type, *nifA*, and *rpoN*$_{1/2}$ mutant cells were complemented with a position-specific frequency matrix-based search for NifA- and σ^{54}-binding sites plus a simple operon definition. One of the newly identified NifA+σ^{54}-dependent genes, *fdxN*, encodes a ferredoxin required for efficient symbiotic nitrogen fixation, which makes it a candidate for being a direct electron donor to nitrogenase. The *fdxN* gene has an unconventional, albeit functional σ^{54} promoter with the dinucleotide GA instead of the consensus GC motif at position –12. A GC-containing mutant promoter and the atypical GA-containing promoter of the wild type were disparately activated. Expression analyses were also carried out with two other NifA+σ^{54} targets (*ectC*; *ahpC*). Incidentally, the tiling-like design of the microarray has helped to arrive at completely revised annotations of the *ectC*- and *ahpC*-upstream DNA regions, which are now compatible with promoter locations. Taken together, the approaches used here led to a substantial expansion of the NifA+σ^{54} regulon size, culminating in a total of 65 genes for nitrogen fixation and diverse other processes.

Keywords Gene chip · NifA · Nitrogen fixation · Symbiosis · σ^{54} · Transcriptomics

Communicated by A. Hirsch.

Electronic supplementary material The online version of this article (doi:10.1007/s00438-007-0246-9) contains supplementary material, which is available to authorized users.

F. Hauser · G. Pessi · C. Weber · N. Rusca · A. Lindemann · H.-M. Fischer · H. Hennecke (✉)
Institute of Microbiology,
Eidgenössische Technische Hochschule,
Wolfgang-Pauli-Strasse 10,
8093 Zürich, Switzerland
e-mail: hennecke@micro.biol.ethz.ch

M. Friberg
Institute of Computational Science,
Eidgenössische Technische Hochschule,
Universitätsstrasse 6, 8092 Zürich, Switzerland

Introduction

The enzymatic conversion of atmospheric nitrogen to ammonia by nitrogenase is an oxygen-sensitive process that demands large amounts of energy and reductant. Therefore, nitrogenase synthesis is only meaningful in an oxygen-protected environment and with a sufficient cellular supply of ATP and reducing equivalents. In transit from free-living cells to nitrogen-fixing bacteroids rhizobia enter such an environment, the host-plant root nodule. Inside nodules, the concentration of free oxygen decreases by a factor of 10,000 down to approximately 25 nM as compared with an aerobic environment (Kuzma et al. 1993), and photosynthates are provided to bacteroids as sources of energy and reductant to fuel the nitrogenase reaction (Prell and Poole 2006). To adjust expression of nitrogen fixation genes to the proper environmental conditions, rhizobia

have evolved complex regulatory networks in which low oxygen serves as a cue for gene expression (Dixon and Kahn 2004). Oxygen-responsive key regulators involved in rhizobial nitrogen fixation are the FixLJ two-component system and the transcriptional activator protein NifA. These regulators are organized hierarchically either in a single cascade as in the alfalfa symbiont *Sinorhizobium meliloti* or in two parallel, largely independent cascades as in *Bradyrhizobium japonicum*, the symbiont of soybean. The oxygen sensing mechanisms of FixLJ and NifA differ (Dixon and Kahn 2004). In free-living culture, the NifA protein is only active at oxygen concentrations below 0.5% in the gas phase (Sciotti et al. 2003).

In *B. japonicum*, NifA synthesis is under the control of yet another two-component regulatory system, RegSR, whose ortholog in *Rhodobacter capsulatus*, RegBA, mediates global redox-regulation of numerous cellular functions (Bauer et al. 1998; Elsen et al. 2004). The RegSR–NifA cascade controls genes directly involved in nitrogen fixation (e.g., *nif* and *fix* genes encoding nitrogenase and accessory functions) and also genes that are either indirectly related to nitrogen fixation (e.g. $groESL_3$) or have no known function in this process (e.g. *nrgA*, *nrgBC*; for references, see Fischer 1994; Nellen-Anthamatten et al. 1998; Sciotti et al. 2003). RNA polymerase containing σ^{54} (RpoN) is needed for transcription from NifA-dependent –24/–12-type promoters (Dixon and Kahn 2004).

In order to unravel the *B. japonicum* NifA+σ^{54} regulon, we have used in the past different genetic and biochemical approaches that have led to the identification of 13 NifA+RpoN-dependent promoters with 27 associated genes (Fischer et al. 1993; Weidenhaupt et al. 1993; Dainese-Hatt et al. 1999; Nienaber et al. 2000; Göttfert et al. 2001; Caldelari Baumberger et al. 2003). In a recent pilot study which was focused on the 410-kb so-called symbiotic gene region (Göttfert et al. 2001) of the 9.1 Mb *B. japonicum* genome (Kaneko et al. 2002), microarray technology was applied as a new tool to demonstrate its potential for the analysis of regulatory networks at a global cellular scale (Herrgard et al. 2004; Hauser et al. 2006).

Here, we report on the most complete characterization of the NifA+σ^{54} regulon by using defined *nifA* and *rpoN* mutants and a custom-made gene chip that is based on the *B. japonicum* whole-genome sequence (Kaneko et al. 2002). The microarray data are further substantiated by integrating results from a computational prediction of binding sites for the NifA and RpoN transcription factors. Using this strategy, we have discovered new NifA+RpoN-dependent genes, including *fdxN* that encodes a symbiotically important ferredoxin. Moreover, we document how the microarray's tiling-like design has helped in the re-annotation of specific genome regions.

Materials and methods

Bacterial strains, plasmids, media and growth conditions

The bacterial strains and plasmids used in this work are listed in Table 1. Luria-Bertani (LB) medium was used for growth of *Escherichia coli*. For microaerobic growth, 5-ml *E. coli* cultures were grown at 30°C in tightly closed screw-capped plastic vials (7 ml total volume) on a test tube roller. Aerobic cultures were grown in 100-ml Erlenmeyer flasks containing 10 ml of medium. When appropriate, antibiotics were used at the following concentrations (μg/ml): kanamycin, 30; tetracycline, 10; chloramphenicol, 20; ampicillin, 200.

PSY medium (Regensburger and Hennecke 1983) supplemented with 0.1% L-arabinose was used for aerobic growth of the *B. japonicum* wild-type strain 110*spc*4 (Regensburger and Hennecke 1983) and mutant strains N50–97 ($rpoN_{1/2}^{-}$; Kullik et al. 1991) and A9 ($nifA^{-}$; Fischer et al. 1986). For anaerobic growth, yeast-extract-mannitol medium (Daniel and Appleby 1972) supplemented with 10 mM KNO_3 was used. Anaerobic cultures were grown in 500-ml rubber-stoppered serum bottles containing 20–200 ml medium and a gas atmosphere consisting of 100% N_2. Although the two mutants had a delay, their growth rates in the exponential phase were not significantly different from the wild type. When appropriate, media for growth of *B. japonicum* cells contained the following concentrations of antibiotics (μg/ml): spectinomycin, 100; streptomycin, 50; kanamycin, 100; tetracycline, 50 (solid media) or 25 (liquid media).

DNA work

Recombinant DNA work was performed according to standard protocols (Sambrook and Russel 2001). *B. japonicum* chromosomal DNA was isolated as described (Hahn and Hennecke 1984).

Construction of translational *lacZ* fusions

To construct translational *lacZ* fusions to the *fdxN* gene, PCR-amplified regions comprising 135 or 484 bp of the region upstream of *fdxN* were ligated to the linearized vector pSUP482 containing a promoterless *lacZ* gene (Table 1). The correct sequence of all inserts was confirmed by sequencing. The constructs pRJ9288 and pRJ9290 were transformed into *E. coli* MC1061 containing either pMC71A (*K. pneumoniae nifA*) or pRJ7553 (*B. japonicum nifA*). Plasmid pRJ9308 was generated by Quikchange mutagenesis of pRJ9284 using standard protocols

Table 1 Bacterial strains and plasmids used in this work

Strain or plasmid	Relevant genotype or phenotype	Source or reference
Escherichia coli		
DH5α	*supE44 ΔlacU169 (ψ80lacZΔM15)hsdR1 recA1 gyrA96 thi-1 relA1*	BRL, Gaithersburg, USA
S17-1	Sm^r Sp^r *hdsR* (RP4-2 *kan::Tn7 tet::*Mu integrated in the chromosme)	Simon et al. (1983)
MC1061	Δ(*lacIPOZY*)X74 $hsdR^-$	Casadaban et al. (1983)
Bradyrhizobium japonicum		
110*spc*4	Sp^r, wild type	Regensburger and Hennecke (1983)
A9	Sp^r Km^r *nifA*::*aphII*	Fischer et al. (1986)
N50-97	Sp^r Km^r Sm^r $rpoN_1$::*aphII* $rpoN_2$::Ω	Kullik et al. (1991)
X16	Sp^r Sm^r *frxA*::Ω	Ebeling et al. (1988)
9288	Sp^r Tc^r *fdxN′–′lacZ* chromosomally integrated	This study
A9288	Sp^r Km^r Tc^r *nifA*::*aphII fdxN′–′lacZ* chromosomally integrated	This study
N9288	Sp^r Km^r Sm^r Tc^r $rpoN_1$::*aphII* $rpoN_2$::Ω *fdxN′–′lacZ* chromosomally integrated	This study
9297	Sp^r Km^r *fdxN*::*aphII* (opposite orientation)	This study
F9279	Sp^r Km^r Sm^r *fdxN*::*aphII* (opposite orientation) *frxA*:: Ω	This study
9305	Sp^r Km^r *ectC::aphII* (opposite orientation)	This study
9307	Sp^r Km^r ORF116-*ectC::aphII* (opposite orientation)	This study
9314	Sp^r Tc^r ORF116′–′*lacZ* chromosomally integrated	This study
A9314	Sp^r Km^r Tc^r *nifA*::*aphII* ORF116′–′*lacZ* chromosomally integrated	This study
N9314	Sp^r Km^r Sm^r Tc^r $rpoN_1$::*aphII* $rpoN_2$::Ω ORF116′–′*lacZ* chromosomally integrated	This study
9315	Sp^r Tc^r chromosomally integrated *ectC′–′lacZ*	This study
A9315	Sp^r Km^r Tc^r *nifA*::*aphII ectC′–′lacZ* chromosomally integrated	This study
N9315	Sp^r Km^r Sm^r Tc^r $rpoN_1$::*aphII* $rpoN_2$::Ω *ectC′–′lacZ* chromosomally integrated	This study
9329	Sp^r Tc^r *fdxN′–′lacZ* (Pm) chromosomally integrated	This study
A9329	Sp^r Km^r Tc^r *nifA*::*aphII fdxN′–′lacZ* (Pm) chromosomally integrated	This study
N9329	Sp^r Km^r Sm^r Tc^r $rpoN_1$::*aphII* $rpoN_2$::Ω *fdxN′–′lacZ* (Pm) chromosomally integrated	This study
Plasmids		
pGEM-T easy	Ap^r, cloning vector	Promega, Madison, USA
pUC19	Ap^r, cloning vector	Norrander et al. (1983)
pSUP480	Tc^r ‘*lacZ* part from pNM480 in pSUP202pol4	H. M. Fischer, unpublished
pSUP481	Tc^r ‘*lacZ* part from pNM481 in pSUP202pol4	H. M. Fischer, unpublished
pSUP482	Tc^r ‘*lacZ* part from pNM482 in pSUP202pol4	H. M. Fischer, unpublished
pSUP202 pol4	Tc^r (pSUP202) part of the polylinker from pBlueskript II KS+ between *Eco*RI and *Pst*I	Fischer et al. (1993)
pMC71A	Cm^r (pACYC184) p_{tet}::$nifA_{Kp}$	Buchanan-Wollaston et al. (1981)
pRJ6126	Ap^r (pGEM-T easy) 870 bp amplicon comprising *B. japonicum* genome sequence from coordinate 1,936,991 to 1,936,129	This study
pRJ7553	Km^r (pACYC177) p_{cat}::$nifA_{Bj}$	Fischer and Hennecke (1987)

Table 1 continued

Strain or plasmid	Relevant genotype or phenotype	Source or reference
pRJ9284	Amp^r (pUC19) 484 bp amplicon comprising *B. japonicum* genome sequence from coordinate 1,904,151 to 1,904,619	This study
pRJ9288	Tc^r (pSUP482) containing the 479 bp *EcoR*I-*Pst*I fragment of pRJ9284	This study
pRJ9290	Tc^r (pSUP482) 135 bp amplicon comprising *B. japonicum* genome sequence from coordinate 1,904,500 to 1,904,619	This study
pRJ9308	Ap^r (pUC19) 484 bp amplicon comprising *B. japonicum* genome sequence from coordinate 1,904,151 to 1,904,619 with AC exchange at position 1,904,566	This study
pRJ9309	Tc^r (pSUP482) containing the 130 bp *EcoR*I-*Pst*I fragment of pRJ9308	This study
pRJ9310	Ap^r (pUC19) 811 bp amplicon comprising *B. japonicum* genome sequence from coordinate 1,904,151 to 1,904,946	This study
pRJ9314	Tc^r (pSUP480) 301 bp amplicon comprising *B. japonicum* genome sequence from coordinate 2,275,307 to 2,275,592	This study
pRJ9315	Tc^r (pSUP481) 644 bp amplicon comprising *B. japonicum* genome sequence from coordinate 2,275,307 to 2,275,935	This study
pRJ9329	Tc^r (pSUP482) 1,060 bp amplicon comprising *B. japonicum* genome sequence from coordinate 1,903,576 to 1,904,619; A to C exchange at position 1,904,565	This study

(Stratagene, La Jolla, USA) and the following mutagenic primers: fdxN_mut_f GTCTGGCACAAGACTTGCTAGC AAGAAACTGTTCCG; fdxN_mut_R CGGAACAGTTTC TTGCTAGCAAGTCTTGTGCCAGAC. After verification by sequencing, the 479 bp *EcoR*I-*Pst*I fragment was cloned into pSUP482 resulting in pRJ9309. For the construction of pRJ9329, two PCR products amplified with the primer pairs fdxN_1582_f CCTCCGCCAGTATTGATTAGG, fdxN_547_R AACTGCAGGTAGGCCATCAGTGCTATT CC (template: pRJ9309) and fdxN_mut_R fdxN_1002_f CGGAATTCAGCTGGACGAGCTATTCGAAGG (template: genomic DNA) were combined by overlapping PCR and cloned into pSUP482. Plasmids pRJ9288 and pRJ9329 were mobilized into the *B. japonicum* wild-type strain 110*spc*4 and mutant strains A9 and N50-97. The correct genomic integration was verified by PCR.

Translational fusions to ORF116 and *ectC* were constructed similarly. Fragments of 644 bp (*ectC*) and 301 bp length (ORF116) were cloned into pSUP481 and pSUP480 respectively, and the resulting plasmids (pRJ9315 and pRJ9314, Table 1) were mobilized into the *B. japonicum* wild type or mutant strains A9 and N50-97. The correct genomic integration in candidate clones was verified by PCR.

Transcript mapping

The transcription start sites of the *fdxN* and *ahpC* genes were mapped by primer extension experiments (Babst et al. 1996; Nienaber et al. 2000) using different priming oligonucleotides (*fdxN*: fdxN_931_r_seq 5′-CGGCATTGGG ACACTCGAAC-3′, fdxN_951_r_seq 5′-GTCGTTCTTCA GGCTAATCG-3′; *ahpC*: pNR24 5′-TTCCTGCGCTTG AAAACCGGGCTTCACGC-3′, pNR25 5′-ATTTCGGTC AGCGTCTCAAACGCACTCTG-3′). Total RNA (9 µg in each reaction for *fdxN*, 10 µg for *ahpC*) from aerobically grown *B. japonicum* wild type and anaerobically grown *B. japonicum* wild type and mutant strains, and 400 units of SuperScript reverse transcriptase (Invitrogen, Carlsbad, CA, USA) were used for the extension reactions which were performed for 1 h at 42°C. Extension products were analyzed on 6% denaturing polyacrylamide gels adjacent to sequencing ladders generated with the same oligonucleotides and plasmid pRJ9310.

β-Galactosidase assay

β-Galactosidase assays were performed as described previously (Fischer et al. 1993).

Construction of *B. japonicum* mutant strains

Mutagenesis of selected genes was done by marker exchange. Briefly, fragments of the 5′ and 3′ flanking regions of *fdxN* (genome coordinates: 1,904,151–1,904,619 [5′ region]; 1,904,788–1,905,565 [3′ region]), *ectC* (genome coordinates: 2,275,047–2,275,935 [5′ region]; 2,276,263–2,277,004 [3′ region]) and ORF116-*ectC* (genome coordinates: 2,275,047–2,275,592 [5′ region]; 2,276,263–2,277,004 [3′ region]) were PCR amplified and cloned into pSUP202pol4. A kanamycin resistance cassette (*aphII*) isolated from pBSL15 (Alexeyev 1995) was inserted between the two *B. japonicum* DNA fragments. The resulting plasmids were mobilized into appropriate *B. japonicum* strains resulting in the mutant strains listed in Table 1. The correct genomic integration of the constructs by double crossover was verified by PCR.

Plant infection test

The symbiotic phenotype of *B. japonicum* strains 9297, F9297, 9305 and 9307 was determined in infections tests using soybean [*Glycine max* (L.) Merr. cv. Williams]. Nitrogenase activity was measured in an acetylene reduction assay (Hahn and Hennecke 1984; Göttfert et al. 1990).

Design of the *B. japonicum* whole-genome gene chip

A high-density oligonucleotide gene chip (BJAPETHa520090) was custom-designed and manufactured by Affymetrix (Santa Clara, CA, USA). The annotation of ORFs and intergenic regions was based on the genome sequence published by Kaneko et al. (2002). In contrast to the usually constant number of probe pairs (PP) per ORF, the number of PP on the BJAPETHa520090 gene chip is variable. For all ORFs shorter than 350 bp, a minimal number of 13 PP was chosen. For all ORFs longer than 2,000 bp, a maximal number of 48 PP was defined. For all the ORFs with a length between 350 and 2,000 bp, the number of PP linearly increases from 13 to 48. To minimize potential cross-hybridization with plant-derived cDNA, when RNA isolated from root nodules will be used in future experiments, all PPs were pruned against the soybean ESTs represented on the commercial Affymetrix soybean array (Soybean Genome Array, Affymetrix, Santa Clara, USA). Intergenic regions longer than 39 bp are probed at a constant distance of 43 bp. Overall, the intergenic regions are probed with 1–58 PP. As controls, 14 additional bacterial genes (e. g. antibiotic resistance genes, reporter genes) and 15 host plant genes (e. g. *G. max* and *Vigna radiata* leghemoglobin and actin cDNA sequences) were included in the chip design. In these controls, the number of PP was also adjusted according the rules described above. All Affymetrix standard controls (119) were included in the array. In addition, 28 of them are represented in duplicate and 14 in triplicate.

RNA isolation, synthesis of cDNA, and hybridization

Cultures of *B. japonicum* were grown to mid exponential phase. For anaerobic cultures grown in YEM medium, mid exponential phase was reached at an OD_{600} of 0.17–0.24. At harvesting time, cultures (40 ml) were immediately transferred into cold tubes containing 0.1 volume of ''stop solution'' (10% phenol, pH 8, in ethanol; Bernstein et al. 2002) or 0.2 volume of RNAprotect solution (Qiagen, Hilden, Germany). After centrifugation for 5 min (10,800*g*; 4°C), the supernatant was decanted and the pellet immediately frozen in liquid nitrogen and stored at –80°C. Total RNA was isolated using the hot phenol extraction procedure described previously (Babst et al. 1996). RNA integrity was checked by agarose gel electrophoresis. Precipitated RNA (100 µg) was treated with 20 units of RQ1 DNase I (Promega, Madison, USA) for 30 min at 37°C in a reaction volume of 200 µl. SUPERase•In^{TM} (100 units; Ambion, Huntingdon, UK) was included in the reaction to inhibit potential RNase activity. RNA samples were cleaned up with RNeasy spin columns (Qiagen), and the eluted RNA was checked again for integrity by agarose gel electrophoresis. The absence of genomic DNA contamination was controlled by PCR using the primers fixR4109F 5′-TTTTCGACTTCGACGAGAGG-3′ and fixR4564R 5′-TCCGAGAATAGCTTGGCAGT-3′. cDNA was synthesized according to the Affymetrix antisense genome array protocol for *E. coli* (http://www.affymetrix.com). For reverse transcription, MMLV reverse transcriptase RNase H minus (Promega, Madison, USA) was used in the supplied reaction buffer. The resulting cDNA was spectrophotometrically quantified and fragmented according to the Affymetrix manual except that the time for fragmentation by DNase I was shortened to 3 min. For control, 200 ng of DNase I-treated cDNA were separated on a 4-to–20% acrylamide gradient gel and stained with SYBR green II (Molecular Probes, Inc., Eugene, OR, USA). Ideally, the fragmented cDNA migrated in a range that corresponded to 50–200 bp of the 50-bp ladder (Fermentas International Inc., Burlington, Canada). The fragmented cDNA was then end-labelled using terminal dexoynucleotidyl transferase (Promega) in combination with the gene chip labelling reagent (Affymetrix). The reaction was incubated for 75 min at 37°C and stopped by the addition of 2 µl of 0.5 M EDTA.

Hybridisation, washing, staining, and scanning were done according to the Affymetrix manual using a gene chip fluidics station 450 (Affymetrix) and a gene chip scanner 3000 (Affymetrix). For hybridization of individual gene chips, 2–2.5 µg of labelled cDNA were used in a total volume of 150 µl hybridization solution, which contained 7% DMSO (Sigma-Aldrich, St. Louis, USA) in addition to the described composition. Hybridization was done overnight at 48°C. For each strain, a minimum of six biological replicates were done.

Data analysis

Signal intensities were detected and analyzed with the Affymetrix gene chip operating software version 1.2 (GCOS; Affymetrix) using the algorithms described in the Affymetrix statistical algorithms description document (http://www.affymetrix.com). Data were globally scaled to a target intensity of 500, and default statistical parameters of GCOS ($\alpha_1 = 0.05$, $\alpha_2 = 0.065$, $\tau = 0.015$, $\gamma 1H = 0.002$, $\gamma 1L = 0.002$, $\gamma 2H = 0.002667$, $\gamma 2L = 0.002667$, Perturbation 1.1) were applied. Signal values from the arrays were then processed using Genespring GX 7.3 (Agilent Technologies, CA, USA). Individual experiments were normalized with the default settings for Affymetrix arrays, i.e., first data transformation to set measurements of below 0.01 to 0.01 followed by a per-chip normalization to the 50th percentile and a per-gene normalization to median. Statistical analysis included only those probe sets which showed in at least one array a present or marginal MAS5 call. The ''Genespring Wilcoxon two-sample rank test'' with a false discovery rate of 0.01 was used to find differentially expressed probe sets. Probe sets which passed the test were then filtered for a fold change factor larger than 2. Probe sets passing all of these filters were considered to be significantly regulated.

For the tiling analyses, the library file from Affymetrix (bpmap) was reconstructed. Signals were analyzed using GTRANS (Affymetrix) with a bandwith of 70. Signal-profiles were visualized in Microsoft Excel.

Genome-wide motif prediction

Intergenic regions were extracted from the *B. japonicum* genome (file: brady.seq as of 26.08.2002; ftp://ftp.kazusa.zor.jp) using the original annotation (file: brady.p.table.xls) in combination with verified gene names from NCBI (file NC_004463.ptt as of 04.12.05; ftp://ftp.ncbi.nih.gov). Genes were grouped into putative operons by applying similar rules as defined by Mwangi and Siggia (2003). Genes that have the same orientation and are separated by ≤ 32 bp are considered to belong to the same operon. The maximally allowed distance was enlarged to 100 bp if the gene names share the same three first letters in their name. Overall, this approach resulted in 1,416 predicted operons comprising a total of 3,866 genes. Intergenic regions (5,925) which are located outside of putative operons were searched for motifs using the Darwin software (Gonnet et al. 2000). The motifs were represented as position-specific frequency matrices (PSFM) which provides a good approximation of protein-DNA interactions (Benos et al. 2002). Sequences used for the construction of the NifA and RpoN PSFMs are shown in Table S6. The PSFM is a matrix consisting of the frequency of each nucleotide at each motif position, based on a collection of known motifs (Table S6). $\sqrt{N}$ pseudocounts (where N is the number of motifs in the PSFM) were used to find new motifs that were similar, but not identical, to the known motifs (Lawrence et al. 1993). The genomic sequence 500 bp upstream of the first gene of each putative operon was searched for the motif PSFM. Because transcriptional start sites were not known for most genes, the translational start codon was used in all cases as a reference. Each (overlapping) sequence of the same length as the profile was scored by multiplying the frequencies from the PSFM: score $= \prod_{i=1}^{n} \mathrm{PSFM}[i, s(i)]$, where n is the length of the PSFM and s is the sequence (of length n) to be scored. The higher the score values the more similar are the sequences to the consensus of the known motif. The threshold value for a significant motif prediction was given by the motif with the lowest score in the PSFM. Combined searches for NifA and RpoN were done by first identifying significant RpoN motifs and then searching upstream of the predicted motif for the best match to the NifA PSFM. Predictions of potential IHF binding sites were done as described above. The two PSFMs were constructed with two sets of IHF binding sites from *E. coli* deposited in the Prodoric database (Munch et al. 2005). One PSFM was constructed with 101 sites of the prodoric IHF matrix (Accession: MX000028), the other with 60 sites of the RegulonDB as implemented in Prodoric.

Results

Design of the whole-genome array

The *B. japonicum* high-density oligonucleotide array BJAPETHa520090 (Affymetrix GeneChip®; Tables S1, S2) was designed on the basis of the genome sequence and the annotation published by Kaneko et al. (2002). The array comprises 18,968 probe sets of which 8,414 probe for annotated open reading frames, RNA genes and various control sequences. Of all 8,317 annotated protein-encoding ORFs, 8,126 are represented by unique probe sets and 88 by mixed (4) or identical (84) probe sets. A total of 206

genes are not represented by unique probe sets mostly because their sequences are too similar to other sequences (Table S3). Among them are genes encoding 114 (putative) transposases, 45 unknown or hypothetical proteins, and 15 RNA-coding genes. In addition, both strands of intergenic regions longer than 39 bp are represented by PPs having an average spacing of 43 nucleotides. Thus, using the combination of probes for intra- and intergenic regions, the array can be regarded as a low-resolution tiling array.

Comparison of anaerobically grown wild-type with *nifA* mutant cells

A prominent activator for *nif* genes and numerous *fix* genes in *B. japonicum* is the oxygen-responsive NifA protein (Fischer 1994). In order to globally assess the NifA regulon, we compared the transcriptome of the wild type with that of the *nifA* mutant strain A9, both grown anaerobically under conditions of nitrate respiration. Out of a total of 323 genes whose expression differed between the two strains, 190 showed a reduced expression in the *nifA* mutant (Table S4, Fig. S1). Among them are 24 of the previously described 27 NifA+RpoN-dependent genes of *B. japonicum*. Two of them (*nrgB*, id93) were not identified by the de novo annotation algorithms used by Kaneko et al. (2002) and, therefore, no probe sets had been designed. For unknown reasons bll1766 (3′ portion of id117; Hauser et al. 2006) was not detected as significantly regulated under the experimental conditions used here.

This leaves 166 newly found genes whose expression was decreased in the *nifA* mutant. Among them, 90 had assigned functions (Fig. S2, Table 2) such as three ferredoxin genes (*fer*3, *fer*2, *fdxN*). Additional NifA-dependent genes include *ectC* (ectoine synthase) and *ahpCD* (alkyl hydroperoxide reductase) which were studied further (see below).

Surprisingly, 133 genes were expressed higher in the *nifA* mutant than in the wild type. More than half of these genes (77) encode unknown or hypothetical proteins. Possibly, this is the consequence of indirect (cryptic) regulatory effects in the mutant.

Comparison of anaerobically grown wild-type with $rpoN_{1/2}$ mutant cells

Given that activation by NifA is dependent on RNA polymerase containing the specialized transcription factor σ^{54}, we performed comparative chip hybridization analysis with cDNA derived from anaerobically grown wild-type and $rpoN_{1/2}$ mutant cells. Out of 225 genes, whose expression differed in this comparison (Table S5, Fig. S1), 193 showed a reduced and 32 an enhanced expression. In addition to the three known genes that were missing in the comparison of the *nifA* mutant with the wild type (see above), the previously described NifA targets *fixR–nifA*, and *gln*II were not among the RpoN-regulated genes. This means that the gene chip experiment with the $rpoN_{1/2}$ mutant detected 21 of the previously known 27 NifA+RpoN-dependent genes. This leaves 172 new genes showing decreased expression in the $rpoN_{1/2}$ mutant, 85 of them being functionally annotated.

One hundred and thirty-eight of the new genes positively regulated by *nifA* were among those that also showed reduced expression in the $rpoN_{1/2}$ mutant, including all genes depicted in Fig. S2 and in Table 2.

Somewhat unexpected was the enhanced expression of 32 open reading frames in the $rpoN_{1/2}$ mutant eight of which were also found to be increased in the *nifA* mutant. Again, this might be the consequence of indirect (cryptic) regulatory effects originating from the mutant genotype, or it reflects indeed a direct repression by free or RNA polymerase-associated σ^{54}.

It is known from studies in *Klebsiella pneumoniae* that genes located downstream of *rpoN* are involved in modulation of RpoN activity (Merrick and Coppard 1989). In *B. japonicum*, homologous genes are located downstream of $rpoN_2$. Because their expression is not altered in the $rpoN_{1/2}$ mutant, polar effects can be excluded, and thus it is unlikely that they caused regulatory effects in the $rpoN_{1/2}$ mutant.

In silico search for RpoN and NifA binding sites

In order to potentially distinguish direct from indirect NifA+RpoN target genes, a genome-wide in silico DNA motif search was performed using position-specific frequency matrices (PSFM) that are based on both previously described and newly identified binding sites for the two transcription factors (Fig. 1, Table S6). To minimize the number of false positive hits, the search was restricted to 500-bp regions located upstream of start codons of annotated genes.

A total of 100 RpoN binding sites (score $\geq 4.1 \times 10^{-6}$) and 195 NifA binding sites (score $\geq 3.02 \times 10^{-7}$) were predicted (Fig. 2, Table S7). The large majority of them (85 and 108, respectively) were located in intergenic regions. The prediction approach re-identified 18 of 21 known RpoN sites and 14 of the 17 known NifA sites (including those at *fdxN* and *ectC* to be described below; Table S7). Known motifs which were not among the predicted sites either were located outside the sequence range defined by our distance constraints, or were associated with a gene annotated by Göttfert et al. (2001) but not by Kaneko et al. (2002). A total of 19 genes were associated with both motifs (Fig. 2, Table S7). Except for *fixR*, which showed no consistent NifA+RpoN-dependent regulation, 18 genes of this group showed significant fold-change

Table 2 Newly identified and previously described NifA+RpoN-dependent genes

Gene no [a]	Predicted operon members [b]	Gene name [c]	Fold change [d]		Description [a]
			nifA	$rpoN_{1/2}$	
Regulated genes with significant NifA and RpoN binding sites (stringent set)					
blr2143			-114.7	-111.5	similar to cytochrome P450-family protein
	blr2144	cyp112	-37.9	-31.3	cytochrome P-450 BJ-1
	blr2145	cyp114	-20.4	-16.8	cytochrome P-450 BJ-3
bll1767		id121	-63.3	-62.1	hypothetical protein
bll1944			-61.0	-37.0	hypothetical protein
blr6951		*modA*	-45.9	-41.5	molybdenum ABC transporter Molybdate-binding protein
	blr6952	*modB*	-17.5	-24.5	molybdenum ABC transporter permease protein
	blr6953	$modC_2$	-3.9	-2.5	molybdenum ABC transporter ATP-binding protein
	blr6955		-2.8	-2.2	unknown protein
blr1755			-43.3	-39.7	R. etli iscN homolog
blr1719		*modB*	-38.3	-20.9	molybdenum transport system permease protein
blr1743		*nifD*	-37.2	-28.2	nitrogenase molybdenum-iron protein alpha chain
	blr1744	*nifK*	-36.2	-27.0	nitrogenase molybdenum-iron protein beta chain
	blr1745	*nifE*	-33.0	-27.0	nitrogenase molybdenum-cofactor synthesis protein
	blr1746	*nifN*	-27.4	-22.3	nitrogenase molybdenum-cofactor synthesis protein
	blr1747	*nifX*	-20.5	-16.8	iron-molybdenum cofactor processing protein
	blr1748	id79	-13.4	-11.9	hypothetical protein
blr1759		*nifB*	-31.9	-24.2	FeMo cofactor biosynthesis protein
	bsr1760	*frxA*	-27.0	-16.2	ferredoxin-like protein
	blr1761	*nifZ*	-12.9	-11.5	iron-sulfur cofactor synthesis protein
blr1850			-30.5	-30.0	unknown protein
	blr1851	id307	-8.7	-9.5	unknown protein
bsr1739		*fdxN*	-26.0	-13.9	Ferredoxin
bll2060		$groES_3$	-23.8	-25.7	GroES3 chaperonin
	bll2059	$groEL_3$	-13.3	-12.5	GroEL3 chaperonin
blr1769		*nifH*	-23.3	-21.1	dinitrogenase reductase protein
bll2085		id877	-16.0	-15.1	hypothetical protein
blr2108		id930	-13.7	-15.4	probable peptide synthetase
blr1954			-11.8	-4.9	unknown protein
blr1992		id631	-2.9	-3.1	unknown protein
blr2725			-2.1	-3.1	hypothetical protein
bll0889			-2.0	-2.6	putative transport protein
Regulated genes with significant RpoN binding site but no closely associated NifA binding site (extended set)					
blr2106[e]		*ectC*[e]	-116.4	-100.7	L-ectoine synthase
bll1906			-76.9	-57.1	N-acetyltransferase NrgA homolog
blr1726		id31	-39.8	-18.0	unknown protein
blr1765		*fer2*	-37.7	-16.4	Ferredoxin
bsr2010			-36.5	-26.3	unknown protein
	blr2011		-20.0	-16.0	unknown protein
bll1872			-23.7	-21.1	hypothetical protein
bll2063		*nrgC*	-20.4	-14.7	phenolhydroxylase homolog
bll6942		*hupS,hupA*	-14.5	-11.0	uptake hydrogenase precursor
	bll6941	*hupB,hupL*	-12.5	-10.3	uptake hydrogenase large subunit
	bll6940	*hupC*	-8.5	-9.9	HupC protein
	bll6939	*hupD*	-6.5	-4.4	HupD protein
bll2067		*nfeC*	-13.6	-12.6	nodulate formation efficiency C protein
bll3193			-8.1	-10.4	unknown protein
bll5734		*nrtA*	-8.0	-6.4	ABC transporter nitrate-binding protein
blr2038		*fixA*	-6.4	-5.8	electron transfer flavoprotein beta chain
blr7289		$luxA_2$	-5.5	-6.0	putative alkanal monooxygenase
blr1971		id587	-5.3	-4.5	putative peptidase
blr6145		*dctA*	-4.9	-4.7	C4-dicarboxylate transport protein
bll2801			-3.3	-3.1	probable potential formate transporter
blr1879		id370	-3.2	-3.2	hypothetical protein
blr0612		*glnK*	-3.2	-2.6	nitrogen regulatory protein PII
	blr0613	*amtB*	-3.3	-3.1	ammonium transporter
blr5374			-3.0	-4.8	hypothetical protein
bll7180			-2.4	-3.3	hydantoin utilization protein
	bll7179		-2.1	-2.5	putative N-methylhydantoinase B
	bll7178		-3.2	-4.9	hypothetical protein
	bll7177		-2.8	-3.5	hypothetical protein
	bll7176		-2.9	-3.3	hypothetical protein
blr2803		*nrtA*	-2.4	-2.4	ABC transporter nitrate-binding protein
bsl2575			-2.3	-3.3	hypothetical protein
Regulated gene with manually identified RpoN and NifA sites					
bll1777		*ahpC*	-52.9	-35.8	alkyl hydroperoxide reductase
	bll1776	*ahpD*	-15.7	-10.5	alkyl hydroperoxide reductase

[a] Information as published by Kaneko et al. (2002). All genes shaded in grey were previously known NifA+RpoN-dependent target genes

[b] Operons were predicted as described in ''Materials and methods''

[c] Gene names as indicated in the EMBL-EBI database

[d] Fold change values of a comparison of anaerobically grown wild-type versus *nifA* mutant cells (*nifA*) or wild-type versus $rpoN_{1/2}$ mutant cells ($rpoN_{1/2}$)

[e] Significant NifA site, which was found by manual inspection, is located outside the 500-bp-window. The new operon structure is ORF116-*ectC* (Fig. 3)

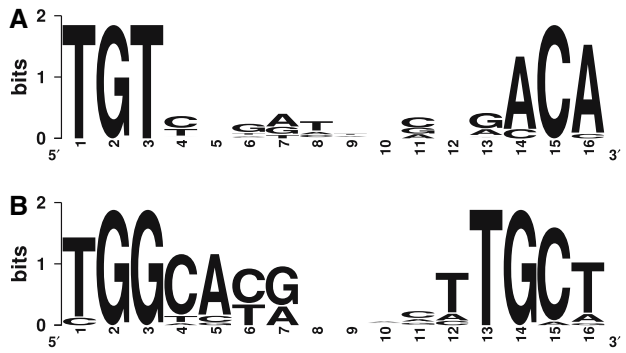

Fig. 1 Sequence logos for NifA (**a**) and RpoN binding sites (**b**) created by using ''WebLogo'' (Crooks et al. 2004). The consensus motifs are based on individual motifs listed in Table S6

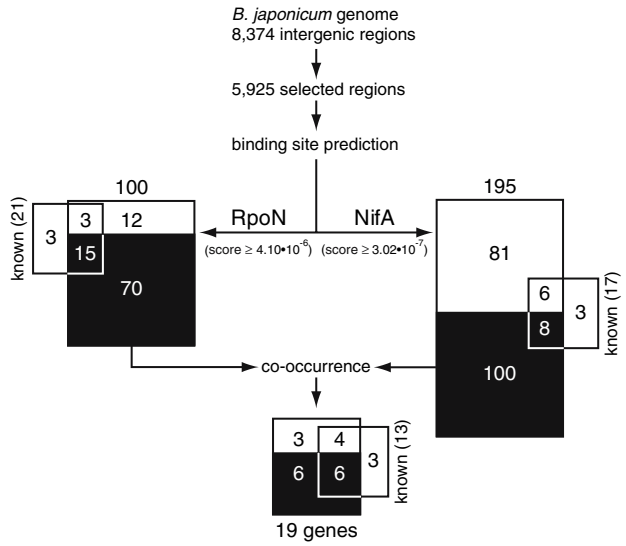

Fig. 2 Work-flow and results of the genome-wide in silico prediction of binding sites for RpoN and NifA in the *B. japonicum* genome. For details, see ''Materials and methods''. The analysis was restricted to intergenic regions (500 bp) upstream of annotated genes or operons. *Numbers above boxes* refer to the total number of predicted sites with a score above the indicated threshold. *Numbers inside vertical rectangles* indicate the number of predicted binding sites located outside (*numbers in white on black background*) or inside of annotated genes or open reading frames located further upstream (*numbers in black on white background*). *Numbers inside squares* refer to binding sites associated with previously identified RpoN- and/or NifA-dependent genes. *Numbers outside squares* refer to previously identified RpoN-binding sites which, however, were not predicted by the algorithm (for further details, see also Table S7)

values in both gene chip experiments with the *rpoN*$_{1/2}$ and *nifA* mutant (stringent set; Table 2, Table S7). Conversely, 22 NifA+RpoN-regulated genes associated with a predicted RpoN site had no significant NifA binding site in close vicinity (extended set, Table 2, Table S7). When the operon definition specified in ''Materials and methods'' was applied to the 40 genes in the combined stringent and extended sets, the number of genes increased to 63, all of them being positively regulated by NifA and RpoN (Table 2, Table S7). Taken together, the sum (63) of the stringent (18) and extended (22) set of genes plus the co-regulated putative operon members (23) most likely represent the direct members of the combined NifA+RpoN regulon of *B. japonicum* (Table 2).

Tiling analysis around *ectC*, and analysis of *ectC* function in symbiosis

The putative ectoine synthase gene *ectC* showed very high fold-change values in both comparative chip experiments. While a well conserved RpoN motif was predicted 426 bp upstream of *ectC*, the NifA binding site predicted within the 500-bp window upstream of *ectC* had only a low score and was located too close to the RpoN core promoter (Table S7). Yet, manual sequence inspection revealed a perfect NifA binding site (TGT-N$_{10}$-ACA; score = 3.8×10^{-6}) located 512 bp further upstream of *ectC*.

We made use of the tiling-like architecture of our array to further analyze the transcriptional profile of this region (Fig. 3a). It turned out that signal intensities increased immediately downstream of the predicted RpoN promoter in the wild type but much less in the *rpoN*$_{1/2}$ and *nifA* mutants, which suggested synthesis of a NifA+RpoN-dependent transcript from this promoter. Inspection of the transcribed, non-annotated region upstream of *ectC* revealed an open reading frame (ORF116 [genome coordinates 2,275,570–2,275,920]; Fig. 3a) coding for a 12.6 kDa protein without significant similarity to any protein in the non-redundant database.

Expression and regulation of ORF116 and *ectC* was studied with translational *lacZ* fusions (Fig. 3b). β-Galactosidase activity measurements with anaerobically grown cells clearly documented that both ORF116 and *ectC* are transcribed and translated, and regulated in an RpoN- and NifA-dependent manner (Fig. 3c).

An *ectC* deletion mutant and an ORF116-*ectC* double deletion mutant (strains 9305 and 9307; Fig. 3b) showed wild-type phenotypes with regard to number and dry weight of nodules and acetylene reduction activity with soybean as host plant (data not shown).

Tiling analysis of the genome region around *ahpCD*

Gene *ahpC*, encoding a potential alkyl hydroperoxide reductase, showed a rather high fold-change in both comparative chip experiments and, based on genomic organization, looked as if it was in an operon with bll1778 and *ahpD* (Fig. 4a). Yet, only *ahpCD*, but not bll1778, was significantly regulated in both mutants compared to wild type, and no significant NifA or RpoN binding site could be

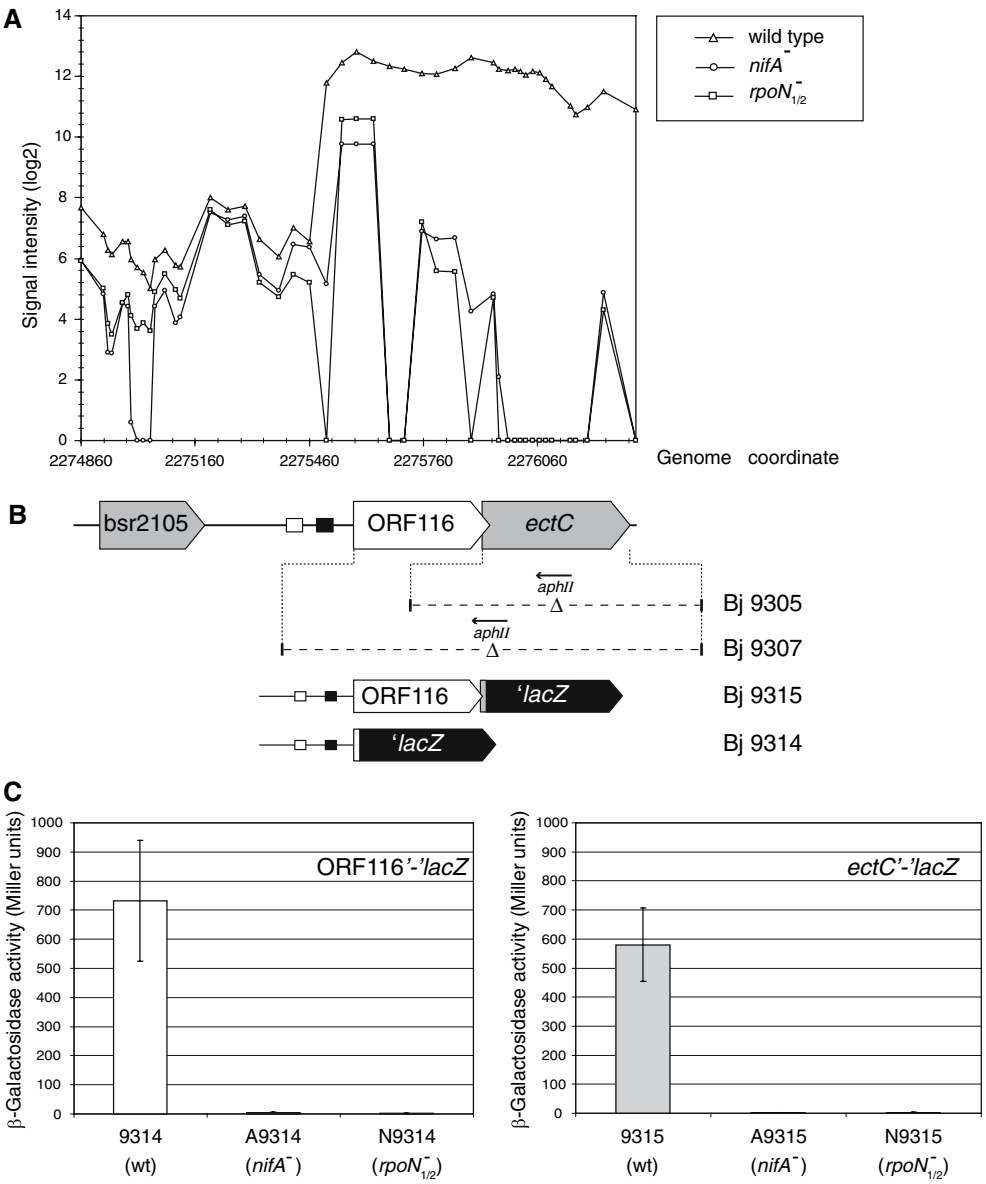

Fig. 3 Transcription analysis of the *B. japonicum ectC* locus. **a** Graphical representation of hybridization signal intensities derived from individual probe pairs of the *ectC* region (for details, see ''Materials and methods''). To improve visualization, individual data points were connected by *solid lines*. Genes annotated by Kaneko et al. (2002) are indicated by *shaded horizontal arrows* below the genome coordinate axis. ORF116 which was annotated in this study, is shown as *white horizontal arrow*. *Open and filled boxes* represent predicted NifA and RpoN sites, respectively. **b** Structure of deletion mutations and *lacZ* fusions generated in this study. Mutations in ORF116 and *ectC* and structures of chromosomally integrated *lacZ* fusions are shown along with the corresponding *B. japonicum* (*Bj*) strain numbers. *Small horizontal arrows* indicate the orientation of the *aphII* (Km^r) cassette used for gene replacement. **c** Expression of translational ORF116′–′*lacZ* and *ectC*′–′*lacZ* fusions in anaerobically grown *B. japonicum* wild-type and mutant strains. Displayed are mean values of *β*-galactosidase activities ± standard errors calculated from at least three independent cultures measured in duplicate

identified upstream of bll1778. The transcript profile of this region suggested the presence of a transcript starting near the end of the bll1778 coding region (Fig. 4a). This transcript was mapped by a primer extension experiment (Fig. 4b) and shown to be present only in the anaerobically grown wild-type but not in *nifA* or $rpoN_{1/2}$ mutants. Its 5′ end was located 12 nucleotides downstream of a significant RpoN binding site (TGGCATATGGTTTGCT, score: 9.9×10^{-6}).

Expression analysis of *fdxN*, a ferredoxin gene

We were interested in substantiating the gene chip data with respect to the NifA and RpoN-dependent expression of *fdxN* because the sequence of the –24/–12 region of the associated putative RpoN promoter is GG-N_{10}-GA instead of the usual GG-N_{10}-GC minimal consensus (marked P in Fig. 5). Primer extension experiment clearly showed that this promoter is functional (Fig. 6).

Regulation of *fdxN* was further analyzed in *E. coli* MC1061 using three translational *lacZ* reporter fusions which differed in the *fdxN* promoter portions (Fig. 5). Constitutively expressed *nifA* genes from either *K. pneumoniae* (pMC71A) or *B. japonicum* (pRJ7553) were provided in trans on a second plasmid. Control strains lacking *nifA* had very low *β*-galactosidase activity regardless of the growth conditions and the extent of the promoter region present (Table 3). The oxygen-insensitive *K. pneumoniae* NifA protein was able to activate the fusion located on pRJ9288 (wild-type promoter) but not on pRJ9290 (lacking

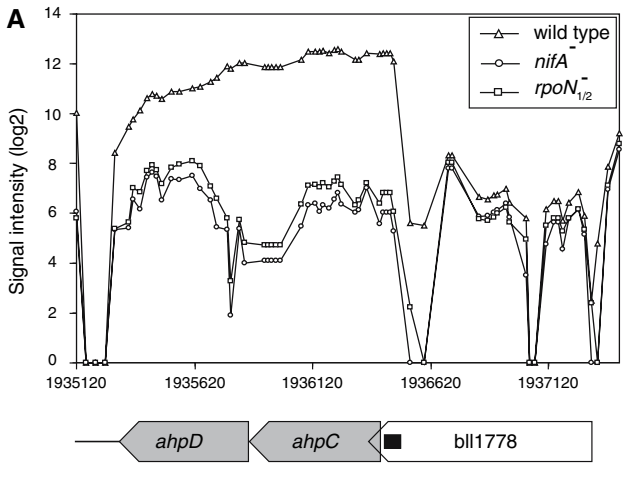

Fig. 4 Transcript analysis of the *B. japonicum ahpC* locus. **a** Graphical representation of hybridization signal intensities derived from individual probe pairs of the *ahpC* region (for details, see ''Materials and methods''). To improve visualization, individual data points were connected by *solid lines*. Genes annotated by Kaneko et al. (2002) are indicated by *horizontal arrows* below the genome coordinate axis. The *black box* within bll1778 indicates the predicted RpoN binding site (TGGCATATGGTTTGCT, score: 9.9×10^{-6}). **b** Transcription start site mapping of *ahpC*. Shown are the extension products obtained with primer pNR24 and RNA isolated from *B. japonicum* wild-type (*wt*) cells, *nifA* mutant (A9) and $rpoN_{1/2}$ mutant (N50–97) cells grown in the absence of oxygen. The same primer was used in combination with plasmid pRJ6126 to generate the sequence ladder. The relevant nucleotide sequence is shown on the *left* with the –24 and –12 regions of the promoter highlighted by *reverse face* and the transcriptional start marked with a *solid arrowhead*. The same transcription start site was determined also with primer pNR25 (data not shown)

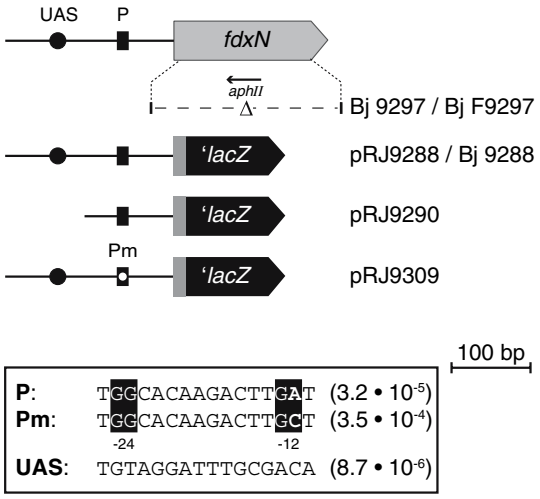

Fig. 5 Structure of the *fdxN* promoter region and plasmid constructs used for its functional analysis. Shown is the structure of the *fdxN* deletion mutant 9297 and that of three translational *fdxN*′–′*lacZ* fusions which differ in their promoter region. Corresponding plasmid and strain numbers are indicated on the *right*. *Small black rectangles* indicate the predicted RpoN-dependent promoter (*P*) which shows an exceptional adenine at position –12. The adenine was replaced by a cytosine in the mutant promoter *Pm*. The *filled circle* indicates the predicted NifA binding site (UAS). The nucleotide sequence of individual binding motifs and their scores are shown in the *box at the bottom*

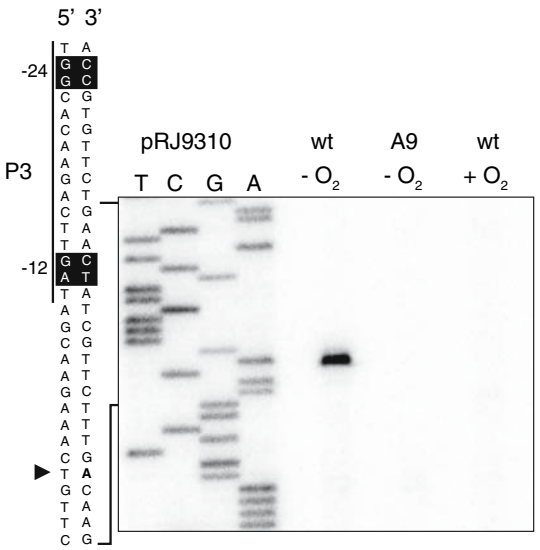

Fig. 6 Transcription start site mapping of *fdxN*. Shown are the extension products obtained with primer fdxN_931_r_seq and RNA isolated from *B. japonicum* wild-type (*wt*) cells grown in the presence ($+O_2$) or absence of oxygen ($-O_2$) and *nifA* mutant (A9) cells grown in the absence of oxygen. The same primer was used in combination with plasmid pRJ9310 to generate the sequence ladder. The relevant nucleotide sequence is shown on the *left* with the –24 and –12 regions of the promoter highlighted by *reverse face* and the transcriptional start marked with a *solid arrowhead*. The same transcriptional start site was determined also with primer fdxN_951_r_seq (data not shown)

UAS), under both aerobic and microaerobic conditions. This result in combination with that of the transcript mapping experiment showed that the predicted NifA binding site was required for transcription activation of the promoter.

In the *E. coli* background, *B. japonicum* NifA was unable to activate *fdxN*′–′*lacZ* expression from any of the reporter

plasmids (Table 3), even under microaerobic conditions which are normally compatible with its oxygen-sensitive activity, as demonstrated in a control experiment with a *nifD′–′lacZ* fusion (data not shown). We reasoned that the atypical –12 region of the promoter might be the cause. To test this hypothesis, we repeated the activation test with the reporter plasmid pRJ9309, which carries a mutated promoter (Pm) where the exceptional A at position –12 had been exchanged by a C that is normally present at this position (Fig. 5).The *fdxN′–′lacZ* fusion preceded by Pm was indeed activated by *B. japonicum* NifA under microaerobic conditions, and activation mediated by *K. pneumoniae* NifA was enhanced approximately 2.5-fold compared with the wild-type promoter present on pRJ9288 (Table 3).

We also investigated *fdxN* regulation in the homologous *B. japonicum* background (Table 3, lower section). Expression of *fdxN′–′lacZ* was anaerobically induced and strictly dependent on both NifA and RpoN, which is in perfect agreement with the gene chip data. Like in the heterologous *E. coli* background, the A_{-12}-to-C exchange in the Pm promoter led to an approximately three-fold increase of promoter activity.

Symbiotic phenotype of *fdxN* and *fdxN-frxA* mutants

The high similarity of FdxN with the previously characterized ferredoxin FrxA (58% identity; Ebeling et al. 1988) suggested that the two proteins may functionally replace each other. For this reason, we not only constructed an *fdxN* mutant (9297; Fig. 5) but also an *fdxN–frxA* double mutant (F9297). Symbiotic properties of the mutant strains were determined in a plant infection test with the soybean host plant. Previous studies with the *frxA* mutant X16 had already shown that this strain displayed almost unaffected wild-type nitrogen fixation (Fix) activity (Ebeling et al. 1988). In contrast, the *fdxN* mutant had a 50% decreased Fix activity as compared with the wild type (Table 4), although the number and dry weight of nodules did not differ. Nodules elicited by the *fdxN–frxA* mutant showed no Fix activity at all.

Table 3 Analysis of *fdxN′–′lacZ* regulation in *E. coli* MC1061 cells expressing *K. pneumoniae* or *B. japonicum* NifA and in *B. japonicum*

Host	Relevant genotype[a]	β-Galactosidase activity[b]	
		Microaerobic[d]	Aerobic
E. coli MC1061[c]			
Plasmid(s)			
pRJ9288	UAS-P	14.3 ± 3.3	8.6 ± 4.4
pRJ9288 + pMC71A	UAS-P $nifA_{Kp}$	349.1 ± 104.4	468.3 ± 143.8
pRJ9288 + pRJ7553	UAS-P $nifA_{Bj}$	25.4 ± 7.2	8.6 ± 3.9
pRJ9290	P	16.3 ± 3.1	8.7 ± 3.2
pRJ9290 + pMC71A	P $nifA_{Kp}$	21.8 ± 2.3	31.4 ± 8.9
pRJ9290 + pRJ7553	P $nifA_{Bj}$	18.5 ± 6.9	9.2 ± 3.3
pRJ9309	UAS-Pm	12.9 ± 4.1	8.3 ± 0.6
pRJ9309 + pMC17A	UAS-Pm $nifA_{Kp}$	973.7 ± 87.5	1,216.3 ± 158.5
pRJ9309 + pRJ7553	UAS-Pm $nifA_{Bj}$	106.0 ± 10.9	10.8 ± 1.3
Strain number		Anaerobic[d]	Aerobic
B. japonicum[c]			
9288	*fdxN′–′lacZ*	732.7 ± 38.8	6.0 ± 6.8
A9288	*fdxN′–′lacZ nifA*$^-$	2.6 ± 0.7	ND
N9288	*fdxN′–′lacZ* $rpoN_{1/2}^-$	4.9 ± 0.7	6.5 ± 7.1
9329	Pm-*fdxN′–′lacZ*	2,425.1 ± 395.4	ND
A9329	Pm-*fdxN′–′lacZ nifA*$^-$	6.3 ± 0.8	ND
N9329	Pm-*fdxN′–′lacZ* $rpoN_{1/2}^-$	6.2 ± 1	ND

Kp, *K. pneumoniae*; *Bj*, *B. japonicum*; *ND*, not determined

[a] The *fdxN* promoter P and Pm are described in the text and depicted in Fig. 5. UAS refers to the predicted NifA binding site upstream of P

[b] Miller units are indicated as mean values ± standard deviation and are derived from at least two independent cultures of individual strains which were assayed at least in duplicate

[c] Note that the *fdxN′–′lacZ* fusion and its derivatives is plasmid-encoded in *E. coli* MC1061 and chromosomally integrated in *B. japonicum*

[d] Microaerobic and anaerobic growth conditions for *E. coli* and *B. japonicum* strains, respectively, are as described in ''Materials and methods''

Table 4 Symbiotic properties of *B. japonicum* ferredoxin mutants

Strain	Relevant genotype	Number of nodules	Nodule dry weight (mg/nodule)	Relative N_2 fixation activity (% of wild type)
110*spc*4	wild type	25 ± 8	1.5 ± 0.4	100 ± 27
9297	Δ*fdxN*	32 ± 11	1.6 ± 0.4	50 ± 7
F9297	Δ*fdxN* Δ*frxA*	30 ± 6	0.7 ± 0.1	0

Discussion

The release of the *B. japonicum* genome sequence (Kaneko et al. 2002) opened the door for constructing a whole-genome array which—in combination with defined mutants lacking either RpoN (σ^{54}) or the transcriptional activator NifA—allowed assessment of the NifA+RpoN regulon by genome-wide transcriptional profiling. The present study with the slow-growing rhizobial species *B. japonicum* complements a number of comparable studies performed most recently with fast-growing rhizobia. Common to all is the purpose to study symbiosis-related genes and the regulons to which they belong (Ampe et al. 2003; Barnett et al. 2004; Becker et al. 2004; Uchiumi et al. 2004; Bobik et al. 2006; Capela et al. 2006).

Global characterization of the *B. japonicum* NifA+RpoN regulon

Prior to this study, 13 NifA+RpoN-dependent *B. japonicum* promoters with a total of 27 associated genes were known which had been identified by different approaches including two-dimensional protein gel electrophoresis (Fischer et al. 1993; Dainese-Hatt et al. 1999), promoter trapping (Weidenhaupt et al. 1993), competitive DNA–RNA hybridization (Nienaber et al. 2000), in silico sequence analysis (Göttfert et al. 2001; Caldelari Baumberger et al. 2003), and gene chip hybridization (Hauser et al. 2006). The latter study as well as a comparable report by Becker et al. (2004) had indicated that the microoxic conditions used for growth were probably not compatible with maximal activity of rhizobial NifA proteins because several of the previously known NifA target genes were not detected as being expressed. For this reason, we have used anaerobic cultures in this work to compare the transcriptomes of the wild type and of *nifA* and *rpoN*$_{1/2}$ mutants. This improvement has yielded confirmation of almost all of the previously known NifA+RpoN targets that are represented on the gene chip. Apart from these, 138 additional genes now showed decreased expression in both mutants, making them candidates for new NifA+RpoN targets. Remarkably, 83 of the 167 genes differentially expressed in both mutants are located in the 410-kb symbiotic region that corresponds to <5% of the entire genome (Göttfert et al. 2001). The functional diversity of these genes adds further evidence to the previous notion that regulation by NifA+RpoN is not restricted to genes encoding nitrogenase and accessory functions but includes many other cellular functions. Hence, NifA in *B. japonicum* might be regarded as a general regulator of anaerobic processes rather than an exclusive transcription factor for nitrogen fixation. Yet, anaerobic nitrate respiration is not controlled by NifA but rather by the FixLJ–FixK$_2$–NnrR cascade (Mesa et al. 2003).

While global transcriptomics did not distinguish between direct or indirect NifA+RpoN target genes or operons, we developed an algorithm for a genome-wide search for RpoN and NifA binding sites that might help zooming in on the direct targets. Using stringent search criteria, this strategy revealed 19 predicted NifA+RpoN-dependent promoters with 34 associated genes of which 32 showed reduced expression in both mutants (Table S7). Seven of the 18 truly regulated, NifA+RpoN-dependent promoters represent previously mapped promoters, whereas 11 were newly identified (Table 2, first section). Summing up all genes associated with the newly identified promoters results in a doubling of the number of genes belonging to the *B. japonicum* NifA+RpoN regulon as compared with previous knowledge.

As it is known that NifA binding sites may be located rather far upstream (Gubler et al. 1989) we also searched for those genes having only an RpoN binding site in the putative promoter region but no significant NifA binding site in close vicinity (relaxed search). With this modification additional putative σ^{54} promoters and their associated genes were predicted. While 94% of all genes found by the stringent search were regulated by NifA and RpoN, the corresponding ratio was only 19% for those genes identified by the relaxed search. Genes in latter group may be activated by NifA bound to a distant site. Similar to what had been described for the RpoN-dependent activator RocR of *Bacillus subtilis* (Belitsky and Sonenshein 1999) these NifA binding sites might also be located within or downstream of these target genes. Yet, this aspect was not covered here. Among the seemingly non-regulated genes of the same group one might expect some that depend on enhancer-binding proteins other than NifA, such as NtrC or DctD or any of the other nine predicted enhancer-binding proteins encoded in the *B. japonicum* genome (Studholme and Dixon 2003; Interpro database; Mulder et al. 2007).

The number of (potential) direct NifA+RpoN target genes derived from the overlap of the chip data with the stringent motif search (32 genes, Table 2) appears quite low if compared with the total number of NifA+RpoN-regulated genes. Yet, the ratio is similar to that found in a comparable study on the ArcBA regulon of *E. coli* where only 58 of 372 regulated genes were associated with one or more predicted ArcA binding sites (Liu and De Wulf 2004). Also, both studies document that there is no correlation between motif score and fold-change values. Thus, promoter sequence information alone is not sufficient to predict transcription efficiency. Also, we did not observe a correlation between relative spacing of predicted NifA- and RpoN-binding sites and differences in the transcript levels.

Additional parameters such as DNA topology or auxiliary factors (e.g., integration host factor; IHF) are indeed known to contribute to promoter strength (Buck et al. 1987; Dixon et al. 1988; Hoover et al. 1990; Bebbington and Williams 2001; Liu et al. 2005). A genome-wide search for IHF sites (details see ''Materials and methods'') revealed that only seven of 18 differentially expressed genes contained a potential IHF motif located between significant NifA and RpoN binding sites (Table S8). Incongruence of predicted and experimentally verified IHF binding sites (*hupS*; Black and Maier 1995) asks for an optimization of the prediction algorithm.

What role for *ectC*?

The *etcC* gene showed high fold-change values in both types of comparative microarray experiments. Its predicted product exhibits 47% amino acid sequence identity to the ectoine synthase of *Marinococcus halophilus*. In this halophilic bacterium, EctC was shown to catalyze the ultimate step in the biosynthesis of the osmoprotectant ectoine (Roberts 2005). The biosynthetic pathway starts from L-aspartate-β-semialdehyde which is converted to ectoine in three subsequent enzymatic steps catalyzed by EctB, EctA and EctC. In *B. japonicum*, however, no obvious homologs for EctB and EctA are present, which raises questions about the functional role of EctC. Our mutational analysis showed that *ectC* is not essential for symbiosis. Even so, it might be possible that a so far unknown substrate of plant or bacterial origin is used by EctC. Hence, we learn from the microarray data with *ectC* that high fold-change values combined with NifA+RpoN dependency do not necessarily guarantee functional relevance of the respective genes in symbiosis.

Towards tiling analyses

Tiling arrays probe for transcribed regions irrespective of annotation, and this information is then used for verification of annotation or even assists *de novo* annotation (Mockler et al. 2005; Samanta et al. 2006). The tiling-like design of the *B. japonicum* array enabled us to detect a new NifA+RpoN-dependent gene, namely the previously non-annotated ORF116 located upstream of *ectC*. Closer analysis of the transcript pattern of additional symbiotic gene regions that were annotated disparately by Göttfert et al. (2001) and Kaneko et al. (2002) indicated that tiling analysis does indeed provide support for one or the other annotation (data not shown). Furthermore, this approach guided us in the identification of the NifA+RpoN-dependent promoter of *ahpC*, which is located within a consistently annotated gene (bll1778, id142). Lack of evidence for transcription of bll1778 itself, the location of the *ahpCD* promoter within it, and absence of similarity of the predicted bll1778 product to known proteins are observations that speak against the existence of bll1778 as a properly annotated gene.

Genome-wide tiling analysis in individual strains was limited by the relatively low resolution of the probes on the *B. japonicum* gene chip and the low signal-to-noise ratio. Yet, by comparing signal profiles between the wild type and *nifA* or $rpoN_{1/2}$ mutant strains it was possible to partially compensate for the signal-to-noise problem, and it is likely that the same strategy can be applied for analyzing other regulatory mutants. Thus, although the restricted resolution of the *B. japonicum* gene chip represents a limitation, we have documented its potential for the tiling analysis of regulated genes.

fdxN, a NifA+RpoN-controlled ferredoxin gene required for symbiotic nitrogen fixation

In contrast to *K. pneumoniae* (Shah et al. 1983), *Anabaena* sp. (Bauer et al. 1993), *R. capsulatus* (Jouanneau et al. 1995) *Rhodospirillum rubrum* (Edgren and Nordlund 2005) little is known about the electron transfer pathway to nitrogenase in *B. japonicum*. In *S. meliloti*, a NifA-controlled ferredoxin (FdxN) was shown to be essential for symbiotic nitrogen fixation (Klipp et al. 1989). The isolation of a ferredoxin from soybean root-nodule bacteroids (Carter et al. 1980), which can function in vitro as electron donor to nitrogenase, provided biochemical support for the role of a ferredoxin in the electron transport pathway to the nitrogenase. The gene chip data presented in this work showed that from a total of 11 *B. japonicum* genes encoding predicted ferredoxins five in fact belong to the NifA+RpoN regulon (*fdxN*, *fer3*, *frxA*, *fer2*, *fixX*). Earlier studies in our laboratory showed that both *frxA* and *fixX* are under the control of NifA (Ebeling et al. 1988; Gubler and Hennecke 1988), and the latter is required for nitrogen fixation. The total amino acid composition of the ferredoxin isolated from bacteroids by Carter et al. (1980) is most similar to that of FdxN and FrxA suggesting a role in

symbiotic nitrogen fixation. The decreased and completely absent Fix activity of the *fdxN* mutant and the *fdxN–frxA* double mutant, respectively, indicate that FdxN is essential for maximal nitrogenase activity and that FrxA can only partially substitute its function. In *R. rubrum*, a model for electron transfer to the nitrogenase was proposed recently, which consists of two parallel pathways that cross-talk to each other at the level of two ferredoxins, FdI and FdN (Edgren and Nordlund 2006). A similar situation may exist in *B. japonicum*, with FixX and FdxN organized hierarchically and FrxA being a component of an alternative electron route to nitrogenase.

Atypical, yet functional –24/–12 promoter of *fdxN*

The NifA+RpoN-dependent promoter of the *B. japonicum fdxN* gene has an atypical –12 region (GA instead of the GC consensus motif). Its identification by our motif search algorithm documents the strength of a weight matrix-based motif search compared with conventional consensus searches. While *fdxN* is the first example of an RpoN-dependent *B. japonicum* gene with a naturally occurring deviation from the –12 GC consensus element, atypical –12 regions have been described previously for the promoters of *nifH* in *Rhizobium leguminosarum*, *Rhizobium leguminosarum* bv *trifolii*, *Rhizobium etli* (Scott et al. 1983; Roelvink et al. 1990; Valderrama et al. 1996) and *glnB* in *R. rubrum* (Johansson and Nordlund 1996). Remarkably, the atypical *fdxN* promoter structure has profound consequences for its ability to be activated by the NifA proteins of *K. pneumoniae* and *B. japonicum* in the *E. coli* background. This result resembles the observation by Buck et al. (1985) who found that a C-to-T or C-to-A exchange at the –12 position of the *K. pneumoniae nifH* promoter had no effect on activation by NifA, yet it abolished (weak) activation by NtrC. Thus, mutations in the –12 position of RpoN-dependent promoters can have activator-specific effects. Moreover, activation of the *fdxN* promoter by the *B. japonicum* NifA protein was host-dependent. This indicates that at this particular promoter, *B. japonicum* NifA requires the homologous transcriptional machinery, which contrasts our previous experience made with numerous other NifA+RpoN-dependent *B. japonicum* promoters that were activated in the heterologous *E. coli* background (Alvarez-Morales and Hennecke 1985; Weidenhaupt et al. 1993). Alternatively, host-dependent activation of the *fdxN* promoter might be explained by the requirement for an additional factor which is present in *B. japonicum* but absent or not functional in *E. coli*.

Acknowledgments Andrea Patrignani, Ralph Schlapbach, Ulrich Wagner from the Functional Genomics Center Zürich (FGCZ) are greatly acknowledged for their contribution to the microarray experiments. We thank Jürg Hauser for programming assistance in the tiling array analysis. Financial support for this work was provided by the Swiss National Foundation for Scientific Research and the ETH through Research Programs for the FGCZ.

References

Alexeyev MF (1995) Three kanamycin resistance gene cassettes with different polylinkers. Biotechniques 18:52–54

Alvarez-Morales A, Hennecke H (1985) Expression of *Rhizobium japonicum nifH* and *nifDK* operons can be activated by the *Klebsiella pneumoniae* NifA protein but not by the product of NtrC. Mol Gen Genet 199:306–314

Alvarez-Morales A, Betancourt-Alvarez M, Kaluza K, Hennecke H (1986) Activation of the *Bradyrhizobium japonicum nifH* and *nifDK* operons is dependent on promoter-upstream DNA sequences. Nucleic Acids Res 14:4207–4227

Ampe F, Kiss E, Sabourdy F, Batut J (2003) Transcriptome analysis of *Sinorhizobium meliloti* during symbiosis. Genome Biol 4:R15

Babst M, Hennecke H, Fischer HM (1996) Two different mechanisms are involved in the heat-shock regulation of chaperonin gene expression in *Bradyrhizobium japonicum*. Mol Microbiol 19:827–839

Barnett MJ, Toman CJ, Fisher RF, Long SR (2004) A dual-genome symbiosis chip for coordinate study of signal exchange and development in a prokaryote-host interaction. Proc Natl Acad Sci USA 101:16636–16641

Barrios H, Grande R, Olvera L, Morett E (1998) *In vivo* genomic footprinting analysis reveals that the complex *Bradyrhizobium japonicum fixRnifA* promoter region is differently occupied by two distinct RNA polymerase holoenzymes. Proc Natl Acad Sci USA 95:1014–1019

Bauer CC, Scappino L, Haselkorn R (1993) Growth of the cyanobacterium *Anabaena* on molecular nitrogen: NifJ is required when iron is limited. Proc Natl Acad Sci USA 90:8812–8816

Bauer E, Kaspar T, Fischer HM, Hennecke H (1998) Expression of the *fixR-nifA* operon in *Bradyrhizobium japonicum* depends on a new response regulator, RegR. J Bacteriol 180:3853–3863

Bebbington KJ, Williams HD (2001) A role for DNA supercoiling in the regulation of the cytochrome *bd* oxidase of *Escherichia coli*. Microbiology 147:591–598

Becker A, Berges H, Krol E, Bruand C, Rüberg S, Capela D, Lauber E, Meilhoc E, Ampe F, de Bruijn FJ, Fourment J, Francez-Charlot A, Kahn D, Kuster H, Liebe C, Pühler A, Weidner S, Batut J (2004) Global changes in gene expression in *Sinorhizobium meliloti* 1021 under microoxic and symbiotic conditions. Mol Plant Microbe Interact 17:292–303

Belitsky BR, Sonenshein AL (1999) An enhancer element located downstream of the major glutamate dehydrogenase gene of *Bacillus subtilis*. Proc Natl Acad Sci USA 96:10290–10295

Benos PV, Bulyk ML, Stormo GD (2002) Additivity in protein-DNA interactions: how good an approximation is it? Nucleic Acids Res 30:4442–4451

Bernstein JA, Khodursky AB, Lin PH, Lin-Chao S, Cohen SN (2002) Global analysis of mRNA decay and abundance in *Escherichia coli* at single-gene resolution using two-color fluorescent DNA microarrays. Proc Natl Acad Sci USA 99:9697–9702

Black LK, Maier RJ (1995) IHF-dependent and RpoN-dependent regulation of hydrogenase expression in *Bradyrhizobium japonicum*. Mol Microbiol 16:405–413

Bobik C, Meilhoc E, Batut J (2006) FixJ: a major regulator of the oxygen limitation response and late symbiotic functions of *Sinorhizobium meliloti*. J Bacteriol 188:4890–4902

Buchanan-Wollaston V, Cannon MC, Beynon JL, Cannon FC (1981) Role of the *nifA* gene product in the regulation of *nif* expression in *Klebsiella pneumoniae*. Nature 294:776–778

Buck M, Khan H, Dixon R (1985) Site-directed mutagenesis of the *Klebsiella pneumoniae nifL* and *nifH* promoters and *in vivo* analysis of promoter activity. Nucleic Acids Res 13:7621–7638

Buck M, Cannon W, Woodcock J (1987) Transcriptional activation of the *Klebsiella pneumoniae* nitrogenase promoter may involve DNA loop formation. Mol Microbiol 1:243–249

Caldelari Baumberger I, Fraefel N, Göttfert M, Hennecke H (2003) New NodW- or NifA-regulated *Bradyrhizobium japonicum* genes. Mol Plant Microbe Interact 16:342–351

Capela D, Filipe C, Bobik C, Batut J, Bruand C (2006) *Sinorhizobium meliloti* differentiation during symbiosis with alfalfa: a transcriptomic dissection. Mol Plant Microbe Interact 19:363–372

Carlson TA, Martin GB, Chelm BK (1987) Differential transcription of the two glutamine synthetase genes of *Bradyrhizobium japonicum*. J Bacteriol 169:5861–5866

Carter KR, Rawlings J, Orme-Johnson WH, Becker RR, Evans HJ (1980) Purification and characterization of a ferredoxin from *Rhizobium japonicum* bacteroids. J Biol Chem 255:4213–4223

Casadaban MJ, Martinezarias A, Shapira SK, Chou J (1983) β-galactosidase gene fusions for analyzing gene expression in *Escherichia coli* and yeast. Methods Enzymol 100:293–308

Chun JY, Stacey G (1994) A *Bradyrhizobium japonicum* gene essential for nodulation competitiveness is differentially regulated from two promoters. Mol Plant Microbe Interact 7:248–255

Chun JY, Sexton GL, Roth LE, Stacey G (1994) Identification and characterization of a novel *Bradyrhizobium japonicum* gene involved in host-specific nitrogen fixation. J Bacteriol 176:6717–6729

Crooks GE, Hon G, Chandonia J-M, Brenner SE (2004) WebLogo: a sequence logo generator. Genome Res 14:1188–1190

Dainese-Hatt P, Fischer HM, Hennecke H, James P (1999) Classifying symbiotic proteins from *Bradyrhizobium japonicum* into functional groups by proteome analysis of altered gene expression levels. Electrophoresis 20:3514–3520

Daniel RM, Appleby CA (1972) Anaerobic-nitrate, symbiotic and aerobic growth of *Rhizobium japonicum*: effects on cytochrome P450, other haemoproteins, nitrate and nitrite reductases. Biochim Biophys Acta 275:347–354

Dixon R, Kahn D (2004) Genetic regulation of biological nitrogen fixation. Nature reviews. Microbiology 2:621–631

Dixon RA, Henderson NC, Austin S (1988) DNA supercoiling and aerobic regulation of transcription from the *Klebsiella pneumoniae nifLA* promoter. Nucleic Acids Res 16:9933–9946

Ebeling S, Noti JD, Hennecke H (1987) Mapping and nucleotide sequence of the *nifS* promoter of *Bradyrhizobium japonicum*. Nucleic Acids Res 15:9598

Ebeling S, Noti JD, Hennecke H (1988) Identification of a new *Bradyrhizobium japonicum* gene (*frxA*) encoding a ferredoxin like protein. J Bacteriol 170:1999–2001

Edgren T, Nordlund S (2005) Electron transport to nitrogenase in *Rhodospirillum rubrum*: identification of a new *fdxN* gene encoding the primary electron donor to nitrogenase. FEMS Microbiol Lett 245:345–351

Edgren T, Nordlund S (2006) Two pathways of electron transport to nitrogenase in *Rhodospirillum rubrum*: the major pathway is dependent on the *fix* gene products. FEMS Microbiol Lett 260:30–35

Elsen S, Swem LR, Swem DL, Bauer CE (2004) RegB/RegA, a highly conserved redox-responding global two-component regulatory system. Microbiol Mol Biol Rev 68:263–279

Fischer HM (1994) Genetic regulation of nitrogen fixation in rhizobia. Microbiol Rev 58:352–386

Fischer HM, Hennecke H (1987) Direct response of *Bradyrhizobium japonicum nifA*-mediated *nif* gene regulation to cellular oxygen status. Mol Gen Genet 209:621–626

Fischer HM, Alvarez-Morales A, Hennecke H (1986) The pleiotropic nature of symbiotic regulatory mutants: *Bradyrhizobium japonicum nifA* gene is involved in control of *nif* gene expression and formation of determinate symbiosis. EMBO J 5:1165–1173

Fischer HM, Babst M, Kaspar T, Acuña G, Arigoni F, Hennecke H (1993) One member of a *groESL*-like chaperonin multigene family in *Bradyrhizobium japonicum* is coregulated with symbiotic nitrogen-fixation genes. EMBO J 12:2901–2912

Fuhrmann M, Hennecke H (1984) *Rhizobium japonicum* nitrogenase Fe protein gene (*nifH*). J Bacteriol 158:1005–1011

Gonnet GH, Hallett MT, Korostensky C, Bernardin L (2000) Darwin v. 2.0: an interpreted computer language for the biosciences. Bioinformatics 16:101–103

Göttfert M, Hitz S, Hennecke H (1990) Identification of *nodS* and *nodU*, two inducible genes inserted between the *Bradyrhizobium japonicum nodYABC* and *nodIJ* genes. Mol Plant Microbe Interact 3:308–316

Göttfert M, Röthlisberger S, Kündig C, Beck C, Marty R, Hennecke H (2001) Potential symbiosis-specific genes uncovered by sequencing a 410-kilobase DNA region of the *Bradyrhizobium japonicum* chromosome. J Bacteriol 183:1405–1412

Gubler M (1989) Fine-tuning of *nif* and *fix* gene expression by upstream activator sequences in *Bradyrhizobium japonicum*. Mol Microbiol 3:149–159

Gubler M, Hennecke H (1988) Regulation of the *fixA* gene and *fixBC* operon in *Bradyrhizobium japonicum*. J Bacteriol 170:1205–1214

Gubler M, Zürcher T, Hennecke H (1989) The *Bradyrhizobium japonicum fixBCX* operon: identification of *fixX* and of a 5′ mRNA region affecting the level of the *fixBCX* transcript. Mol Microbiol 3:141–148

Hahn M, Hennecke H (1984) Localized mutagenesis in *Rhizobium japonicum*. Mol Gen Genet 193:46–52

Hauser F, Lindemann A, Vuilleumier S, Patrignani A, Schlapbach R, Fischer HM, Hennecke H (2006) Design and validation of a partial-genome microarray for transcriptional profiling of the *Bradyrhizobium japonicum* symbiotic gene region. Mol Genet Genomics 275:55–67

Herrgard MJ, Covert MW, Palsson BO (2004) Reconstruction of microbial transcriptional regulatory networks. Curr Opin Biotechnol 15:70–77

Hoover TR, Santero E, Porter S, Kustu S (1990) The integration host factor stimulates interaction of RNA polymerase with NifA, the transcriptional activator for nitrogen fixation operons. Cell 63:11–22

Johansson M, Nordlund S (1996) Transcription of the *glnB* and *glnA* genes in the photosynthetic bacterium *Rhodospirillum rubrum*. Microbiology 142:1265–1272

Jouanneau Y, Meyer C, Naud I, Klipp W (1995) Characterization of an *fdxN* mutant of *Rhodobacter capsulatus* indicates that ferredoxin I serves as electron donor to nitrogenase. Biochim Biophys Acta 1232:33–42

Kaluza K, Hennecke H (1984) Fine structure analysis of the *nifDK* operon encoding the α and β subunits of dinitrogenase from *Rhizobium japonicum*. Mol Gen Genet 196:35–42

Kaneko T, Nakamura Y, Sato S, Minamisawa K, Uchiumi T, Sasamoto S, Watanabe A, Idesawa K, Iriguchi M, Kawashima K, Kohara M, Matsumoto M, Shimpo S, Tsuruoka H, Wada T, Yamada M, Tabata S (2002) Complete genomic sequence of nitrogen-fixing symbiotic bacterium *Bradyrhizobium japonicum* USDA110. DNA Res 9:189–197

Klipp W, Reiländer H, Schlüter A, Krey R, Pühler A (1989) The *Rhizobium meliloti fdxN* gene encoding a ferredoxin-like protein

is necessary for nitrogen fixation and is cotranscribed with *nifA* and *nifB*. Mol Gen Genet 216:293–302

Kullik I, Fritsche S, Knobel H, Sanjuan J, Hennecke H, Fischer HM (1991) *Bradyrhizobium japonicum* has two differentially regulated, functional homologs of the σ^{54} gene (*rpoN*). J Bacteriol 173:1125–1138

Kuzma MM, Hunt S, Layzell DB (1993) Role of oxygen in the limitation and inhibition of nitrogenase activity and respiration rate in individual soybean nodules. Plant Physiol 101:161–169

Lawrence CE, Altschul SF, Boguski MS, Liu JS, Neuwald AF, Wootton JC (1993) Detecting subtle sequence signals—a Gibbs sampling strategy for multiple alignment. Science 262:208–214

Liu X, De Wulf P (2004) Probing the ArcA-P modulon of *Escherichia coli* by whole genome transcriptional analysis and sequence recognition profiling. J Biol Chem 279:12588–12597

Liu YJ, Hu B, Zhu JB, Shen SJ, Yu GQ (2005) *nifH* promoter activity is regulated by DNA supercoiling in *Sinorhizobium meliloti*. Acta Biochim Biophys Sin (Shanghai) 37:221–226

Martin GB, Thomashow MF, Chelm BK (1989) *Bradyrhizobium japonicum glnB*, a putative nitrogen-regulatory gene, is regulated by NtrC at tandem promoters. J Bacteriol 171:5638–5645

Merrick MJ, Coppard JR (1989) Mutations in genes downstream of the *rpoN* gene (encoding σ^{54}) of *Klebsiella pneumoniae* affect expression from σ^{54}-dependent promoters. Mol Microbiol 3:1765–1775

Mesa S, Bedmar EJ, Chanfon A, Hennecke H, Fischer HM (2003) *Bradyrhizobium japonicum* NnrR, a denitrification regulator, expands the FixLJ–$FixK_2$ regulatory cascade. J Bacteriol 185:3978–3982

Mockler TC, Chan S, Sundaresan A, Chen H, Jacobsen SE, Ecker JR (2005) Applications of DNA tiling arrays for whole-genome analysis. Genomics 85:1–15

Mulder NJ, Apweiler R, Attwood TK, Bairoch A, Bateman A, Binns D, Bork P, Buillard V, Cerutti L, Copley R, Courcelle E, Das U, Daugherty L, Dibley M, Finn R, Fleischmann W, Gough J, Haft D, Hulo N, Hunter S, Kahn D, Kanapin A, Kejariwal A, Labarga A, Langendijk-Genevaux PS, Lonsdale D, Lopez R, Letunic I, Madera M, Maslen J, McAnulla C, McDowall J, Mistry J, Mitchell A, Nikolskaya AN, Orchard S, Orengo C, Petryszak R, Selengut JD, Sigrist CJ, Thomas PD, Valentin F, Wilson D, Wu CH, Yeats C (2007) New developments in the InterPro database. Nucleic Acids Res 35:D224–D228

Munch R, Hiller K, Grote A, Scheer M, Klein J, Schobert M, Jahn D (2005) Virtual footprint and PRODORIC: an integrative framework for regulon prediction in prokaryotes. Bioinformatics 21:4187–4189

Mwangi M, Siggia E (2003) Genome wide identification of regulatory motifs in *Bacillus subtilis*. BMC Bioinformatics 4:18

Nellen-Anthamatten D, Rossi P, Preisig O, Kullik I, Babst M, Fischer HM, Hennecke H (1998) *Bradyrhizobium japonicum* $FixK_2$, a crucial distributor in the FixLJ-dependent regulatory cascade for control of genes inducible by low oxygen levels. J Bacteriol 180:5251–5255

Nienaber A, Huber A, Göttfert M, Hennecke H, Fischer HM (2000) Three new NifA-regulated genes in the *Bradyrhizobium japonicum* symbiotic gene region discovered by competitive DNA-RNA hybridization. J Bacteriol 182:1472–1480

Norrander J, Kempe T, Messing J (1983) Construction of improved M13 vectors using oligodeoxynucleotide-directed mutagenesis. Gene 26:101–106

Noti JD, Folkerts O, Turken AN, Szalay AA (1986) Organization and characterization of genes essential for symbiotic nitrogen fixation from *Bradyrhizobium japonicum* I110. J Bacteriol 167:774–783

Prell J, Poole P (2006) Metabolic changes of rhizobia in legume nodules. Trends Microbiol 14:161–168

Regensburger B, Hennecke H (1983) RNA polymerase from *Rhizobium japonicum*. Arch Microbiol 135:103–109

Roberts M (2005) Organic compatible solutes of halotolerant and halophilic microorganisms. Saline Syst 1:5

Roelvink PW, Harmsen M, van Kammen A, van den Bos RC (1990) The *nifH* promoter region of *Rhizobium leguminosarum*: nucleotide sequence and promoter elements controlling activation by NifA protein. Gene 87:31–36

Samanta MP, Tongprasit W, Istrail S, Cameron RA, Tu Q, Davidson EH, Stolc V (2006) The transcriptome of the sea urchin embryo. Science 314:960–962

Sambrook J, Russel DW (2001) Molecular cloning: a laboratory manual. Cold Spring Harbor Laboratory Press, Cold Spring Harbor

Sciotti MA, Chanfon A, Hennecke H, Fischer HM (2003) Disparate oxygen responsiveness of two regulatory cascades that control expression of symbiotic genes in *Bradyrhizobium japonicum*. J Bacteriol 185:5639–5642

Scott KF, Rolfe BG, Shine J (1983) Biological nitrogen fixation: primary structure of the *Rhizobium trifolii* iron protein gene. DNA 2:149–155

Shah VK, Stacey G, Brill WJ (1983) Electron transport to nitrogenase. Purification and characterization of pyruvate:flavodoxin oxidoreductase, the *nifJ* gene product. J Biol Chem 258:12064–12068

Simon R, Priefer U, Pühler A (1983) Vector plasmids for *in vivo* and *in vitro* manipulation of gram-negative bacteria. In: Pühler A (ed) Molecular genetics of the bacteria–plant interaction. Springer, Heidelberg, pp 98–106

Studholme DJ, Dixon R (2003) Domain architectures of σ^{54}-dependent transcriptional activators. J Bacteriol 185:1757–1767

Uchiumi T, Ohwada T, Itakura M, Mitsui H, Nukui N, Dawadi P, Kaneko T, Tabata S, Yokoyama T, Tejima K, Saeki K, Omori H, Hayashi M, Maekawa T, Sriprang R, Murooka Y, Tajima S, Simomura K, Nomura M, Suzuki A, Shimoda Y, Sioya K, Abe M, Minamisawa K (2004) Expression islands clustered on the symbiosis island of the *Mesorhizobium loti* genome. J Bacteriol 186:2439–2448

Valderrama B, Davalos A, Girard L, Morett E, Mora J (1996) Regulatory proteins and *cis*-acting elements involved in the transcriptional control of *Rhizobium etli* reiterated *nifH* genes. J Bacteriol 178:3119–3126

Weidenhaupt M, Fischer HM, Acuña G, Sanjuan J, Hennecke H (1993) Use of a promoter-probe vector system in the cloning of a new NifA-dependent promoter (*ndp*) from *Bradyrhizobium japonicum*. Gene 129:33–40